Report

Cell Reports

Antivirulence Properties of an Antifreeze Protein

Graphical Abstract

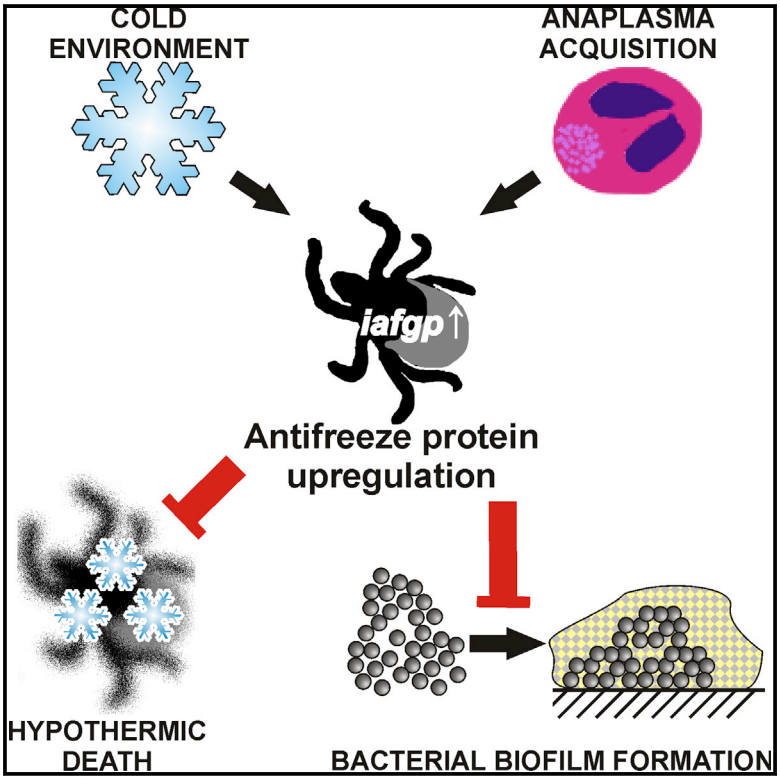

Highlights

The antifreeze protein IAFGP protects against cold damage and bacterial infection

IAFGP is sufficient to confer resistance against multiple pathogens, including MRSA

IAFGP is the first antivirulence factor targeting only bacterial biofilm formation

The homologous peptide P1 phenocopies IAFGP function in vivo

Authors

Martin Heisig, Nabil M. Abraham, ..., Herve Agaisse, Erol Fikrig

Correspondence

martin.heisig@yale.edu (M.H.),
erol.fikrig@yale.edu (E.F.)

In Brief

Heisig et al. show that IAFGP, a tick antifreeze glycoprotein that was known to confer cold resistance, also functions as a potent antivirulence factor during infection. IAFGP prevents bacterial biofilm formation in multiple pathogens, and a homologous synthetic peptide shows potential for application in medical applications.

Heisig et al., 2014, Cell Reports 9, 417–424
October 23, 2014 ©2014 The Authors
http://dx.doi.org/10.1016/j.celrep.2014.09.034

Cell Reports
Report

Antivirulence Properties of an Antifreeze Protein

Martin Heisig,[1,6,*] Nabil M. Abraham,[1,4,6] Lei Liu,[1,6] Girish Neelakanta,[1,6,7] Sarah Mattessich,[1] Hameeda Sultana,[1,7] Zhengling Shang,[1] Juliana M. Ansari,[1] Charlotte Killiam,[1] Wendy Walker,[1,8] Lynn Cooley,[2] Richard A. Flavell,[3,4] Herve Agaisse,[5] and Erol Fikrig[1,4,*]
[1]Department of Internal Medicine, Section of Infectious Diseases, Yale University School of Medicine, New Haven, CT 06520, USA
[2]Department of Genetics, Yale University School of Medicine, New Haven, CT 06520, USA
[3]Department of Immunobiology, Yale University School of Medicine, New Haven, CT 06520, USA
[4]Howard Hughes Medical Institute, Chevy Chase, MD 20815, USA
[5]Department of Microbial Pathogenesis, Yale University School of Medicine, New Haven, CT 06520, USA
[6]Co-first author
[7]Present address: Department of Biological Sciences, Old Dominion University, Center for Molecular Medicine, Norfolk, VA 23529, USA
[8]Present address: University Health Sciences Center, Texas Tech University, El Paso, TX 79905, USA
*Correspondence: martin.heisig@yale.edu (M.H.), erol.fikrig@yale.edu (E.F.)
http://dx.doi.org/10.1016/j.celrep.2014.09.034

SUMMARY

As microbial drug-resistance increases, there is a critical need for new classes of compounds to combat infectious diseases. The *Ixodes scapularis* tick antifreeze glycoprotein, IAFGP, functions as an antivirulence agent against diverse bacteria, including methicillin-resistant *Staphylococcus aureus*. Recombinant IAFGP and a peptide, P1, derived from this protein bind to microbes and alter biofilm formation. Transgenic *iafgp*-expressing flies and mice challenged with bacteria, as well as wild-type animals administered P1, were resistant to infection, septic shock, or biofilm development on implanted catheter tubing. These data show that an antifreeze protein facilitates host control of bacterial infections and suggest therapeutic strategies for countering pathogens.

INTRODUCTION

Diverse ectotherms tolerate the cold by altering the temperature at which their tissues freeze or by preventing the damage caused by the formation of ice (Doucet et al., 2009). Major mechanisms of cold adaptation include the accumulation of solvents to lower the freezing point and the synthesis of antifreeze proteins (AFPs) that bind ice crystals (Davies and Sykes, 1997). AFPs prevent the growth of ice crystals in a noncolligative manner, lowering the freezing point of the solution. Additional properties of AFPs include the inhibition of ice recrystallization or cell membrane stabilization at low temperatures (Davies and Sykes, 1997; Venketesh and Dayananda, 2008). Antifreeze glycoproteins (AFGPs), a class of AFPs, are characterized by canonical Ala-Ala-Thr (AAT) or Pro-Ala-Thr (PAT) repeats with a β-D-galactosyl-(1→3)-α-N-acetyl-D-galactosamine disaccharide attached to each threonine (Carvajal-Rondanelli et al., 2011). Arctic fish AFGPs contain between 4 and 55 repeats, and AFGPs of different length may synergize, suggesting functional differences encoded into the number of tripeptide repeats and spacer sequences between them (Garner and Harding, 2010).

Ixodes scapularis ticks are seasonally exposed to cold temperatures in northern latitudes (Brownstein et al., 2003). We recently identified an *I. scapularis* AFGP, named IAFGP (Neelakanta et al., 2010). *iafgp* expression in ticks and in *iafgp*-transgenic fruit flies correlated with increased survival at low temperatures (Neelakanta et al., 2010, 2012). Interestingly, *iafgp* expression in the tick was upregulated, both in the cold and upon infestation with a common *I. scapularis*-borne pathogen, *Anaplasma phagocytophilum*, the agent of human granulocytic anaplasmosis (Neelakanta et al., 2010). Expression of *iafgp* did not diminish the *A. phagocytophilum* burden within ticks (Neelakanta et al., 2010). Overall, these data suggest a form of mutualism, in which a microbe enhances the capacity of its arthropod vector to survive in the cold, thereby indirectly increasing its own potential to be transmitted to a vertebrate host. For some plant AFPs, chitinase or glucanase activity has been shown in vitro, suggesting that these proteins may have additional properties (Griffith and Yaish, 2004; Huang and Duman, 2002; Meyer et al., 1999; Yaish et al., 2006; Zhang et al., 2007). Here we investigate the influence of IAFGP on infection with *Staphylococcus aureus* and other bacteria in vitro and in vivo.

RESULTS

In Vitro Activity of IAFGP

IAFGP contributes to *I. scapularis* and *Drosophila melanogaster* resistance against cold stress (Neelakanta et al., 2010, 2012). Here we examine whether IAFGP is also involved in the host-pathogen response. Recombinant glutathione S-transferase (GST)-tagged IAFGP, but not GST alone, bound to various bacteria, purified peptidoglycan was sufficient for IAFGP binding (Figures 1A and 1B). In vitro, the addition of GST-IAFGP did not alter planktonic growth of the microbes; however, it strongly interfered with biofilm formation in static *S. aureus* cultures (Figures 1C and S1A). Although mock- or GST-treated bacteria established a biofilm in glucose-supplemented medium, GST-IAFGP-treated microorganisms showed significantly reduced biofilm formation (Figure 1C; $p < 0.001$). Immunoblot data demonstrated decreased amounts of the exopolysaccharide poly-N-acetylglucosamine (PNAG), a major biofilm component,

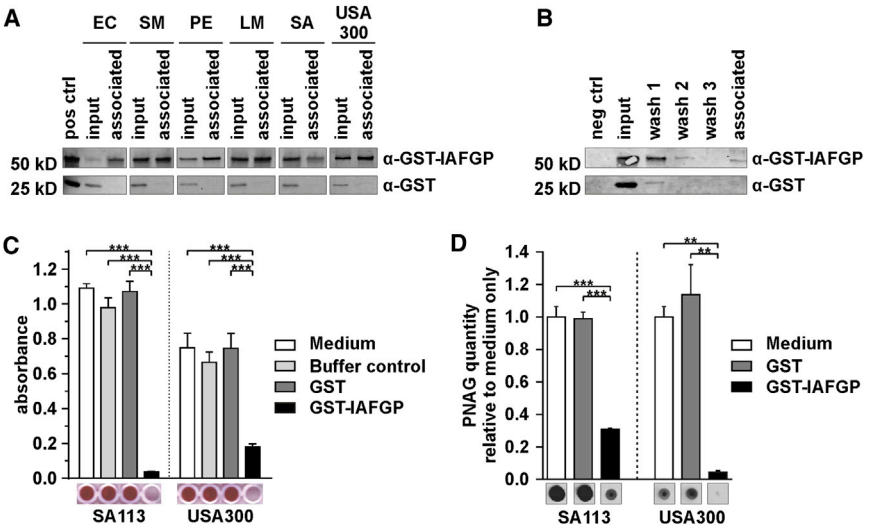

Figure 1. IAFGP Binds Bacteria and Alters Microbial Biofilm Formation In Vitro

(A) *Escherichia coli* (EC), *Serratia marcescens* (SM), *Pseudomonas entomophila* (PE), *Listeria monocytogenes* (LM), *Staphylococcus aureus* SA113 (SA), or *Staphylococcus aureus* USA300 JE2 (USA300) were incubated with recombinant GST or GST-IAFGP (input). Bound protein (associated) was detected by immunoblot analysis. Recombinant GST-IAFGP or GST alone was used as positive control respectively (pos ctrl).

(B) Insoluble *S. aureus* peptidoglycan was incubated with recombinant GST or GST-IAFGP (input), respectively, and wash fractions (wash1–3) and the peptidoglycan-containing pellet (associated) were probed for protein content by immunoblot analysis. Without protein incubation peptidoglycan showed no detectable signal (neg ctrl).

(C) Biofilm formation of *S. aureus* cultures supplemented with GST or GST-IAFGP was measured using Safranin stains. In addition to *S. aureus* SA113, the methicillin-resistant USA300 JE2 isolate was investigated. Results are means ± SEM of three independent experiments performed in duplicate, with representative images of the stained biofilm below (one-way ANOVA with Tukey's posttest). Bacteria cultured in BHI/G (Medium) or supplemented with protein purification elution buffer (Buffer control) served as controls.

(D) PNAG levels of *S. aureus* SA113 and the USA300 JE2 isolate supplemented with GST or GST-IAFGP were assessed using immunoblot analysis. Results are means ± SEM of three independent experiments (one-way ANOVA with Tukey's posttest). Bacteria cultured in BHI/G (medium) without protein addition were used as reference.

in bacteria exposed to GST-IAFGP (Figure 1D; $p < 0.001$). Similar to a prototypic *S. aureus* strain (SA113), a methicillin-resistant *S. aureus* (MRSA) isolate (USA300), which is an important drug-resistant organism that causes substantial clinical disease, also bound GST-IAFGP, resulting in biofilm and PNAG suppression (Figures 1A, 1C, and 1D; $p < 0.001$ and $p < 0.01$).

The vast majority of the primary amino acid sequence of IAFGP contains highly conserved peptide repeats. Except for the predicted N-terminal secretion signal, IAFGP is composed of repeats consisting of the canonical AFGP amino acid triplets AAT and PAT interspersed between a six amino acid spacer sequence Pro-Ala-Arg-Lys-Ala-Arg (PARKAR), approximately every 21 amino acids (Figure S1B). Eight of the 10 IAFGP repeats share a high level of identity, and the other two show variations in the spacer sequence. We therefore investigated whether individual repeats might also be involved in antimicrobial activity. We synthesized a peptide (P1) with hallmarks of this domain, including a PARKAR spacer followed by six AAT triplets, to investigate this region's binding affinity for bacteria and antimicrobial activity (Figure S1C). We chose *S. aureus* as a model organism, as it is a gram-positive pathogen of great clinical importance. We extended our studies to *Listeria monocytogenes*, *Pseudomonas entomophila*, and *Serratia marcescens* to include an additional gram-positive agent and gram-negative microbes. Similar to the full-length protein, P1 bound to different bacterial species (Figure 2A). Peptide binding competed with IAFGP for binding to the microbes, while scrambled P1 (sP1) served as a control (Figure 2B). Likewise to IAFGP, P1 abrogated *S. aureus* biofilm formation and PNAG levels under static culture conditions, but did not influence bacterial viability (Figures 2C, 2D, and S1D; $p < 0.001$ and $p < 0.001$). These data demonstrate that IAFGP and P1 directly bind gram-positive and gram-negative pathogens and have antibiofilm properties.

iafgp-Expressing *D. Melanogaster* Show Resistance to Bacterial Infection

iafgp-expressing *D. melanogaster* (Neelakanta et al., 2012) were used to study the anti-infective activity of IAFGP in invertebrates. Fly infection by microinjection with *S. aureus* showed enhanced survival in comparison to controls (Figure 3A; $p < 0.001$). Needle prick infection with *L. monocytogenes* or oral infection with *S. marcescens* or *P. entomophila* also showed increased survival of *iafgp*-transgenic flies, indicating a broad spectrum of protection (Figures S2A–S2C; $p < 0.05$, $p < 0.001$, and $p < 0.001$). To discriminate between tolerance or resistance mechanisms causing the increase in survival, the pathogen load was quantified. The bacterial burden in control flies increased for 4 days, demonstrating microbial growth. In contrast, the pathogen titers in *iafgp*-expressing flies remained stable over the course of infection, indicating either reduced replication or growth homeostasis with host-induced killing (Figure 3B). Bacterial titers in transgenic and control flies showed significant differences 2–4 days after challenge, suggesting that IAFGP is involved in infection resistance (Figure 3B; $p < 0.001$, $p < 0.01$, and $p < 0.05$).

We then assessed whether increased resistance of *iafgp*-expressing flies to *S. aureus* was due to a more efficient host response to infection or a direct effect on the bacteria. Fly immunity is comprised of three innate effector mechanisms. Hemocytes similar to macrophages engulf pathogens, antimicrobial peptides (AMPs) exert direct bactericidal effects, and melanin deposition leads to microbe encapsulation (Kim and Kim, 2005). All effector mechanisms contribute to the response against a *S. aureus* challenge (Nehme et al., 2011). Blocking fly phagocytosis or melanization during *S. aureus* infection affected survival of *iafgp*-expressing and control flies to a similar extent

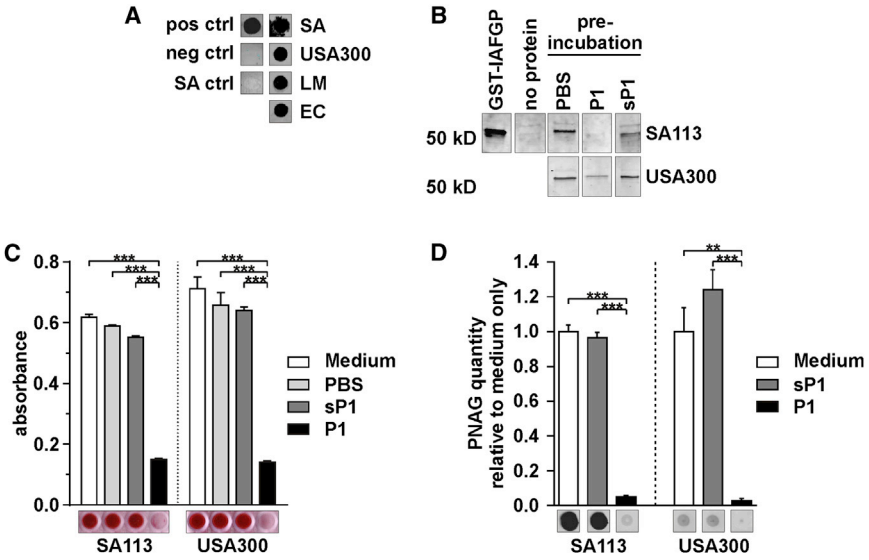

Figure 2. Binding of P1 to *Staphylococcus Aureus* Interferes with Biofilm Formation In Vitro

(A) *S. aureus* SA113, the methicillin-resistant USA300 JE2 isolate, *L. monocytogenes* EGDe, and *E. coli* DH5α were incubated with biotinylated P1 (pos ctrl) in DMSO. Following washing, bound peptide was detected by immunoblot. DMSO or SA113 without peptide incubation served as negative controls.

(B) *S. aureus* SA113 and USA300 were pre-incubated in PBS supplemented with P1 or sP1 before incubation with GST-IAFGP. Following removal of unbound GST-IAFGP, GST-IAFGP associated with the bacterial pellet was detected by immunoblot. Recombinant GST-IAFGP was used as positive control for immunoblot.

(C) Biofilm formation of *S. aureus* SA113 and USA300 JE2 cultures supplemented with P1 or sP1 were measured with Safranin stains. Results are means ± SEM of three independent experiments performed in quadruplicate; representative images of the biofilm stain are shown (one-way ANOVA with Tukey's posttest). Bacteria cultured in BHI/G (Medium) or supplemented with PBS serve as controls.

(D) PNAG formation of *S. aureus* supplemented with P1 or sP1 was visualized by immunoblot. Results are means ± SEM of three independent experiments, with representative images of the stained biofilm (one-way ANOVA with Tukey's posttest). Bacteria cultured in BHI/G (Medium) without protein addition were used as reference.

(Figures S3A and S3B; $p < 0.001$, $p < 0.001$) and AMP expression levels were not increased by IAFGP (Figure S4), suggesting that the anti-infective function of IAFGP was not mediated through a direct effect on fly immunity. Consistent with the in vitro observations, the PNAG quantity during *S. aureus* infection was reduced in *iafgp*-expressing flies compared with controls (Figure 3C; $p < 0.001$). Immunohistochemical detection of *S. aureus* and PNAG in infected flies confirmed diminished bacterial colonization and the decrease in PNAG (Figure 3D). When flies were challenged with a PNAG-deficient *S. aureus ΔicaADBC* mutant, the protective effect of IAFGP was completely abrogated (Figure 3E). These data show that the anti-infective function of IAFGP in flies correlates with bacterial PNAG synthesis on *S. aureus* challenge.

iafgp-Expressing Mice Show Increased Survival following Bacterial Challenge and Sepsis

As IAFGP shows anti-infective activity in vitro and in an invertebrate model of infection, we assessed whether IAFGP has a similar function in vertebrates. We generated a transgenic mouse line expressing *iafgp* ubiquitously (Figure S5A). Mice were subjected to cecal ligation and puncture (CLP), a well-characterized model of polymicrobial sepsis (Rittirsch et al., 2009). We observed increased survival of *iafgp*-expressing mice in comparison to controls after CLP surgery, reflected by a 35% extended average survival time (Figure 4A; $p < 0.05$). Hypothermia was delayed, and serum cytokine release of MCP-1, a marker of sepsis, was reduced in *iafgp*-expressing mice compared with control animals (Figures 4B and S5B; $p < 0.001$). The transgenic animals also recorded significantly better general health and activity at 24–36 hr after surgery than control mice (Figure 4C; $p < 0.05$). A monomicrobial intranasal challenge with MRSA also demonstrated enhanced survival of *iafgp*-transgenic mice compared with controls (Figure 4D; $p < 0.05$). Collectively, these results show that IAFGP affords protection for mice against bacterial infection.

Coating of Catheter Biomaterial with P1 Prevents Biofilm Formation

Staphylococci are responsible for half of the catheter-related bloodstream infections in the United States (Maki et al., 2006; Ramos et al., 2011). *S. aureus* accounts for at least 20% of these infections and is associated with high morbidity and mortality (Walz et al., 2010). To investigate whether IAFGP or P1 interfere with bacterial attachment to biomaterials, we incubated intravenous catheters in protein or peptide solution and then transferred them into *S. aureus* suspensions. IAFGP and P1 spontaneously associated with the catheters and reduced biofilm formation (Figure 5A). Associated bacteria were lowered 9- and 40-fold, respectively, in comparison to untreated controls (Figure 5A; $p < 0.05$). To investigate biofilm formation in vivo, P1-coated catheters were implanted subcutaneously into mice and inoculated with *S. aureus*. Seventy-two hours later, the catheters were removed and examined for bacterial attachment and biofilm formation. P1-coated catheters demonstrated a 40-fold reduction in the number of attached bacteria in comparison to mock-treated catheters (Figure 5B; $p < 0.001$). Scanning electron microscopy further showed that catheters coated with P1 had a marked reduction of PNAG in *S. aureus* biofilms (Figure 5C). The altered biofilm formation on biomaterials confirmed the in vivo activity of P1 and suggests its application as prophylactic coating to prevent bacterial attachment.

DISCUSSION

These data collectively demonstrate the antivirulence properties of an AFP. Bacterial binding of IAFGP or P1 correlated with

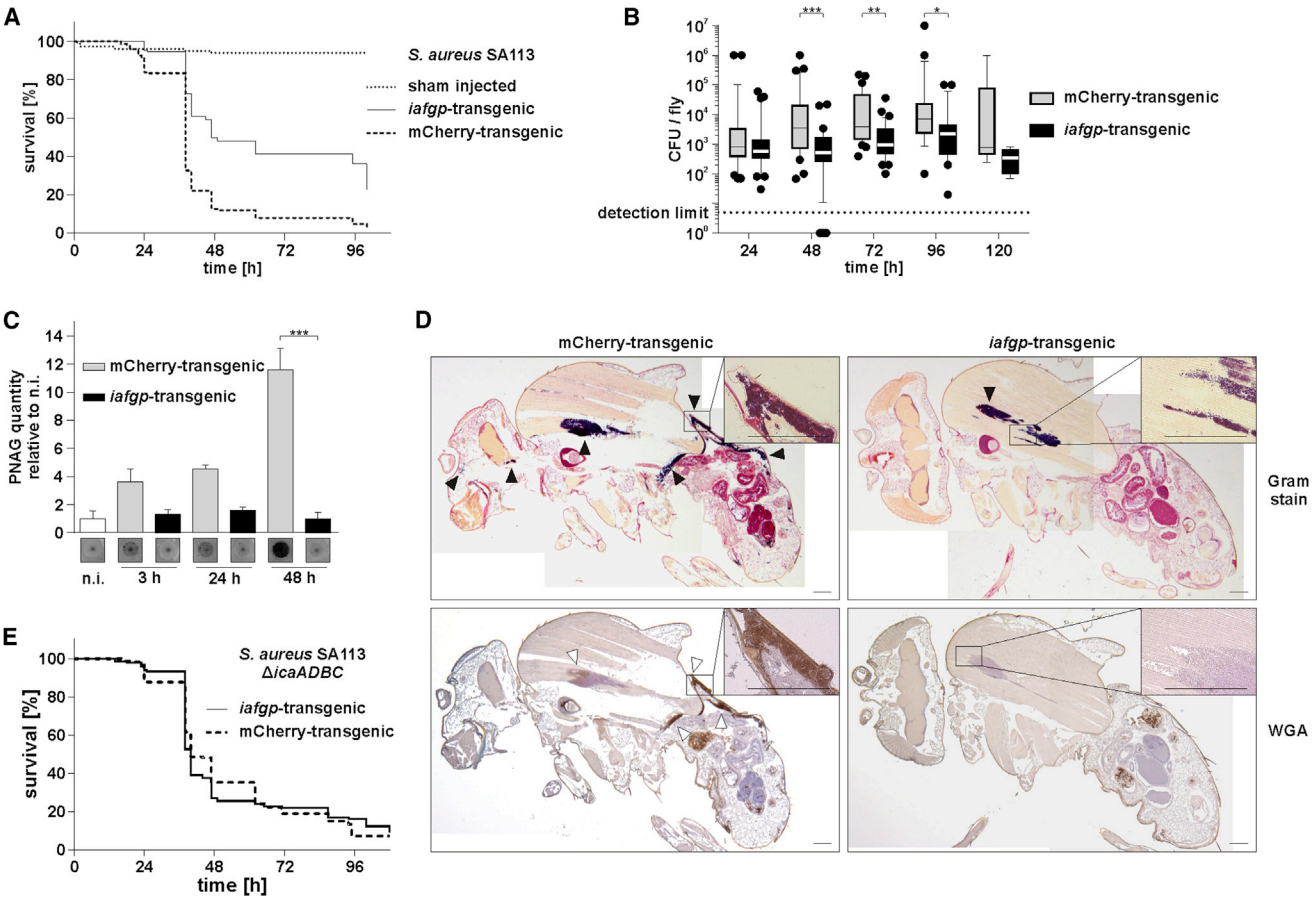

Figure 3. *iafgp* Expression Reduces *Drosophila* Susceptibility to *Staphylococcus Aureus* Challenge In Vivo

(A) *iafgp*-transgenic and mCherry control flies (n = 150/180) were challenged with 500–1,000 CFU *S. aureus* SA113. Sham animals received PBS injections only. Survival data were pooled from three independent experiments (log rank test).

(B) *iafgp*-transgenic and control flies were challenged with 50–100 CFU *S. aureus* SA113. Bacterial colonization of individual flies was determined by plating serial dilutions. Data were pooled from three independent experiments. Box plot extends from the 25th to 75th percentiles, whiskers from the 10th to 90th percentiles, the line inside the box represents the median CFU (two-way ANOVA with Sidak's posttest).

(C) *iafgp*-transgenic and control flies were challenged with 500–1,000 CFU *S. aureus* SA113. PNAG levels of pools of five flies were assessed at different time points by immunoblot. Relative signal intensity to noninfected (n.i.) flies is shown. Average signal intensities of three independent experiments ± SEM with representative immunoblot images are shown (two-way ANOVA with Sidak's posttest).

(D) *iafgp*-transgenic and control flies were challenged with 500–1,000 CFU *S. aureus* SA113. Paraffin sections of whole flies 24 hr postinfection were stained for bacteria (Gram stain) and PNAG (WGA, brown color). Black triangles point to bacteria; white triangles indicate PNAG. Inlet pictures show a magnified area with individual bacterial cells; the scale bar length is 100 μm.

(E) *iafgp*-transgenic and control flies (n = 150/180) were challenged with 500–1,000 CFU *S. aureus* SA113 Δ*icaADBC*, deficient in PNAG production. Survival data were pooled from four independent experiments (log rank test).

inhibition of biofilm formation *in S. aureus* and translated into increased host survival following bacterial challenge. Since expression of genes encoding exopolysaccharide (PNAG) formation was not decreased (Figure S5C), we postulate that binding of IAFGP or P1 interferes with envelope structure or associated proteins, affecting cellular signaling or PNAG secretion and assembly.

S. aureus exopolysaccharide protects bacteria against attacks of the host response by inactivating phagocytic cells and providing a barrier against bactericidal compounds, such as AMPs or antibiotics (Vuong et al., 2004; Nishimura et al., 2006). Immunocompromised flies lacking AMP expression did not benefit from *iafgp* during infection (data not shown). Together these data suggest that IAFGP binding to *S. aureus* and the associated reduction in biofilm formation lead to a greater susceptibility of the pathogen to the immune response of the fly host but not an altered immune response, supporting the antivirulence function of IAFGP.

In warm-blooded animals, a drop of the body core temperature in response to cold environments results in cell damage and death before tissues freeze (Boutilier, 2001; Long et al., 2005). Collectively, our data show that an AFP has antivirulence activity, mediated by rendering the bacteria more susceptible to immune clearance following the prevention of biofilm formation.

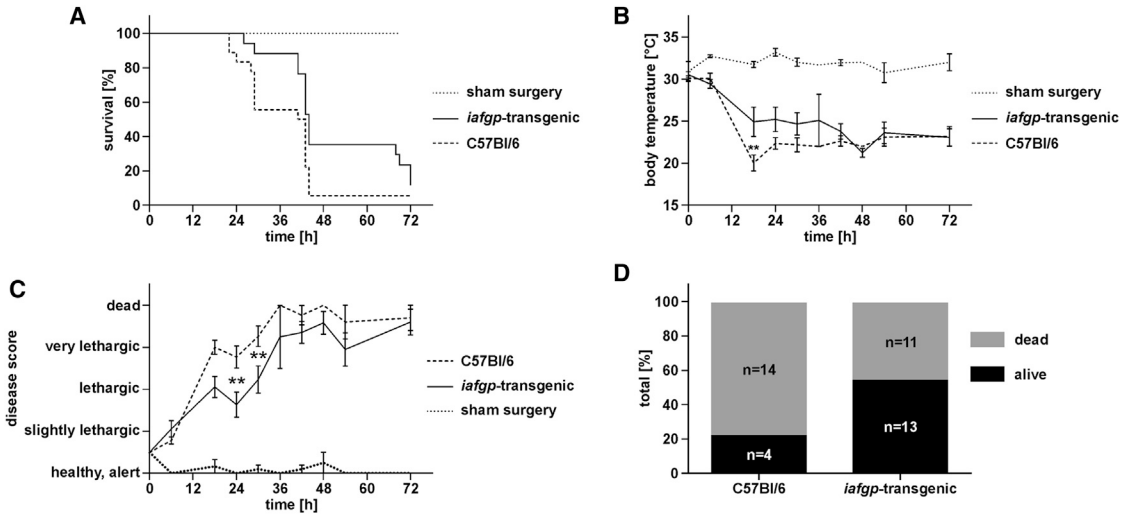

Figure 4. *iafgp*-Expressing Mice Show Increased Resistance to Polymicrobial Sepsis or *Staphylococcus Aureus* USA300 JE2 Challenge

(A–C) *iafgp*-transgenic mice and C57Bl/6 wild-type animals (n = 15/16) underwent CLP surgery. Results were pooled from five independent experiments. Mice of both genotypes (n = 5), receiving sham surgery without CLP, were used as controls. (A) Murine survival (log rank test), (B) body temperature (two-way ANOVA with Sidak's posttest), and (C) disease score (two-way ANOVA with Sidak's posttest) are shown.

(D) *iafgp*-transgenic mice and C57Bl/6 wild-type animals (n = 24/18) were challenged intranasally with *S. aureus* USA300 JE2. Pooled mouse survival of two independent experiments at 36 hr after infection is shown (chi-square test).

In ectotherms, low environmental temperatures cause a reduction of the body temperature, therefore limiting available energy due to diminished nutrient uptake and metabolic activity (Turk, 2010; Storey and Storey, 2013). As these organisms cool they become less effective at combatting pathogens (Bouma et al., 2013; Triggs and Knell, 2012). Moreover, when organisms warm after a period of cooling, they may remain more susceptible to bacterial infection until they have increased their temperature and regained their optimal metabolic activity. From an evolutionary perspective, it would be beneficial if a molecule that facilitated survival in the cold also afforded protection against microorganisms. IAFGP represents the first identified broad-spectrum antivirulence protein, and it will be interesting to determine whether other classes of (antifreeze) proteins also exhibit this activity (Allen et al., 2014). These studies also have substantial practical implications and suggest therapeutic strategies to prevent or control bacterial disease in humans, including infections associated with implanted biomaterials, either directly or in synergy with traditional antibiotics.

EXPERIMENTAL PROCEDURES

Cloning, Expression, and Purification of IAFGP

iafgp lacking the predicted secretion signal was PCR amplified from pGEMT-iafgp (Neelakanta et al., 2010) using oligomers pGEX-F and pGEX-RL, digested with EcoRI and XhoI and cloned into pGEX-6p-3 (GE Healthcare). Protein expression was induced with 1 mM IPTG for 3 hr at 37°C, and bacteria were lysed using a French pressure cell press at 20,000 pounds per square inch. Following centrifugation, GST-IAFGP was affinity purified using GST Sepharose (GE Healthcare), eluted (elution buffer; 50 mM Tris-HCl, 10 mM reduced glutathione [pH 8.0]), and stored in aliquots at −80°C. Precision protease treatment or dialysis resulted in IAFGP degradation. Therefore, the GST-tagged protein in elution buffer was used for experiments. Recombinant GST was purified from pGEX-6p-3 following the same protocol and used as a control.

Protein/Peptide Binding Assays and Immunoblot Analysis

One to 2 × 10^7 *E. coli* DH5α, *S. marcescens* Db11 (GFP), *P. entomophila* (GFP), *L. monocytogenes* EGDe, *S. aureus* SA113, or *S. aureus* USA300 JE2 in stationary growth phase were washed, resuspended in 100 μl PBS or DMSO (Life Technologies; assays involving biotinylated P1 were performed in 100% DMSO; Sigma-Aldrich), and recombinant GST, GST-IAFGP, or biotinylated peptide was added (1.6 μM and 0.9 μM or 6.9 μM final concentration, respectively). Supernatant was removed after 10 min incubation at 37°C, and the pellet was washed three times in 0.1% Triton X-100 (Sigma-Aldrich) in PBS or in 100% DMSO. Proteins were mixed with loading dye, heat denatured, and size separated by SDS-PAGE. Immunoblot using a polyclonal murine serum raised against GST-IAFGP or GST monoclonal antibody (Sigma-Aldrich) was used for specific protein detection. Peptide samples were spotted on polyvinylidene fluoride membrane, dried, and probed with infrared (IR)-labeled streptavidin (LI-COR). The LI-COR Odyssey system was used to visualize IR-labeled secondary probes (LI-COR). To investigate peptidoglycan binding, 28 μg *S. aureus* peptidoglycan (Sigma-Aldrich) were incubated for 10 min with recombinant GST-IAFGP, GST, or biotinylated P1 (416 μM) in PBS or DMSO, respectively, and washed three times, and bound protein or peptide was detected as described above. The impact of peptide preincubation on IAFGP binding to bacteria was investigated. Following incubation of washed bacteria for 30 min at 37°C with 0.2 mg/ml peptide (92.7 μM; KECK Biotechnology Resource Laboratory; heat dissolved in PBS), the bacterial pellet was washed three times in 0.1% Triton X-100 in PBS, and IAFGP binding was assayed as described above. PNAG detection was performed as described using rabbit antisera against PNAG (Cramton et al., 1999). In brief, following incubation of *S. aureus* with proteins or peptides, PNAG was released into the supernatant by boiling in 0.5 M EDTA. Proteins were digested by Proteinase K treatment. Finally, insoluble components were sedimented by centrifugation before loading the samples on nitrocellulose membranes for detection by immunoblot.

Static Biofilm Assay

Biofilm assays were performed as described (Christensen et al., 1985). In brief, planktonic overnight cultures of *S. aureus* were diluted in glucose-supplemented tryptic soy broth or brain-heart infusion broth (1% glucose) to OD_{600} = 0.015 and distributed into 96 well plates (Corning). Plates were

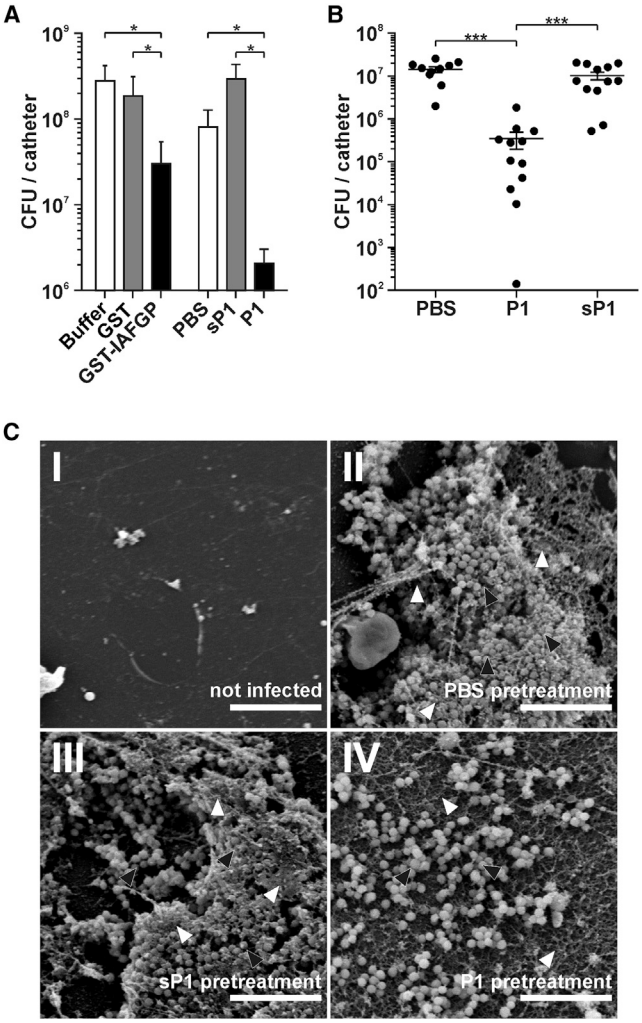

Figure 5. P1 Associates with Intravenous Catheters and Restricts *Staphylococcus Aureus* Biofilm Formation In Vitro and In Vivo

(A) Intravenous catheter tubing was preincubated in protein elution buffer (Buffer) supplemented with GST or GST-IAFGP or in PBS supplemented with P1 or sP1 before transferring into *S. aureus* SA113 suspensions. Bacterial attachment was quantified after sonication by plating serial dilutions. Average CFU values pooled from three independent experiments ± SEM are shown (protein and peptide data: one-way ANOVA with Tukey's posttest).

(B) Intravenous catheters were incubated for 24 hr in PBS, P1, or sP1 and washed and implanted subcutaneously into the dorsal flanks of C57Bl/6 mice (n = 5/6/6); 72 hr after catheter inoculation with 5×10^5 CFU *S. aureus* SA113, the catheters were removed, and the attached bacteria were quantified by plating serial dilutions. CFU data were pooled from three independent experiments. Each data point represents one catheter (one-way ANOVA with Tukey's posttest).

(C) Scanning electron microscopic analysis of catheters 72 hr postimplant. The catheter shown in I was removed from an uninfected mouse. Catheters in II–IV were pretreated with PBS, peptide sP1, or peptide P1, respectively, before implant and *S. aureus* inoculation. *S. aureus* is indicated by black triangles and the biofilm matrix by white triangles. Scale bar, 10 μm.

incubated for 18 hr at 37°C, and bacterial growth in each well was confirmed by the measurement of OD_{600} using a spectrophotometer (BioTek). The supernatant was discarded, and the wells were washed with water twice. Bacteria associated with the well surface were dried and stained with safranin. The dye was then dissolved in 33% acetic acid and the absorbance quantified at 415 nm using a spectrophotometer (BioTek). Bacterial attachment on catheter material preincubated with peptides was also investigated in biofilm assays. Vialon TM catheters (BD Biosciences) were incubated for 18 hr in peptides dissolved in PBS (46 μM), washed with PBS, and incubated in stationary bacterial suspensions (OD_{600} = 0.015) for 24 hr. Following removal of nonadherent bacteria with repeated washing, adherent bacteria and biofilms were dissociated using sonication in PBS. Bacterial titers were quantified by plating serial dilutions on agar plates and were calculated as colony-forming units (CFUs) per catheter.

Microscopy

Bacterial infection and PNAG detection in *D. melanogaster* was visualized using Carnoy's fixed and paraffin-mounted specimens; 4 μm sections were rehydrated according to standard protocol and gram stained for bacterial detection. Biotinylated, succinylated wheat germ agglutinin (WGA; 3μg / ml; Vector Labs) was used for PNAG detection, but also showed limited cross-reactivity to components of the bacterial cell wall at higher concentrations (data not shown). Binding was visualized using the Vectastain ABC Kit and ImmPACT DAB peroxidase substrate (Vector Labs) and was counterstained with Hematoxylin QS (Vector Labs). Scanning electron microscopy was used to investigate biofilm formation on explanted catheters. Following surgical removal and a single washing step in PBS, the catheters were fixed for 1 hr at 23°C in 4% glutaraldehyde solution, washed three times in PBS, and additionally fixed for 1 hr at 23°C in 2% osmium tetroxide solution. Following repeated washing in water, the samples were dehydrated using increasing concentrations of ethanol, dried in liquid CO_2 and sputter coated using the EMS 550X (EMS). Images were acquired using the ISI SS40 (International Scientific Instruments) operating at 10 kV.

Mouse Immunization and Antibody Generation

Polyclonal murine sera against recombinant GST-IAFGP were generated by subcutaneous immunization of female 6–8 week old Balb/c mice with 5 μg GST-IAFGP in Freund's complete adjuvant. Mice were boosted twice every 8–10 days with Freund's incomplete adjuvant and sacrificed 10 days after the final immunization. Polyclonal sera were used for detection of IAFGP.

Fly Propagation and Fly Infection

The iafgp-expressing and *mCherry*-expressing flies were generated as described (Neelakanta et al., 2012). *D. melanogaster* were maintained using standard procedures (Bownes et al., 1990). The fly colony was sustained at 21°C–23°C. Following infection, flies were incubated at 29°C to increase upstream activation sequence-mediated transgene expression. Five- to 9-day-old females were used for experiments. Twenty to 30 flies per vial were infected by microinjection as reviewed (Apidianakis and Rahme, 2009), and survival was monitored. Microinjection was performed into the thorax below the wing using a Nanojet microinjector (Drummond Scientific). Bacteria in stationary growth phase were diluted in PBS to OD_{600} = 0.1, and 9.2 nl were injected, corresponding to an infectious dose of 500–1,000 CFU per fly, respectively. Individual flies injected with an infectious dose of 50–100 CFU were homogenized in 500 μl PBS using a bullet blender and steel beads (Next advance). Serial dilutions were plated on brain-heart infusion agar plates and incubated at 37°C overnight. Endogenous fly bacteria only grew to pinprick size overnight, allowing visual distinction of the fast-growing bacteria used for infection (data not shown). PNAG was detected in pools of five flies. Following homogenization in 200 μl PBS, the supernatant was assayed with immunoblot protocols described above.

Generation of an *iafgp*-Expressing Mouse Line

iafgp was constitutively expressed under control of the chicken β-*actin* promoter in an *iafgp*-transgenic mouse line. The promoter region was excised from pβAct-CAT 9 (ATCC) using XhoI and HindIII and subcloned into the pEGFP-1 vector (Clontech). EGFP was removed from pβAct-EGFP-1 by digestion with BamHI and NotI, resulting in pβAct-1. *iafgp* was then PCR amplified with oligomers *iafgp* BamHI F and *iafgp* NotI R and pGEMT-*iafgp* (Neelakanta et al., 2010) as template, introducing the corresponding restriction sites. The PCR fragment was digested and cloned into linearized pβAct-1, resulting in

pβAct-*iafgp*. For microinjection, the transgene fragment containing the β-*actin* promoter and *iafgp* gene was excised from pβAct-*iafgp* by digestion with XhoI and AflII restriction enzymes and gel purified. Microinjection was performed in 4- to 5-week-old hybrid mouse embryos (C57Bl/6 × C3H), and mice were genotyped by PCR analysis of tail biopsies using IAFP4qRTF and IAFP4qRTR. Full-length *iafgp* amplicons were confirmed, and mRNA expression in multiple tissues was determined using the primers that were used for qRT-PCR. Transgenic *iafgp*-expressing mice were backcrossed for eight generations to C57Bl/6 mice (Charles River). Heterozygous or homozygous experimental mice of 6–12 weeks were age and sex matched with wild-type littermates and wild-type C57Bl/6 as control. All mice were housed at 20°C–22°C with water and food ad libitum. Animal handling was performed according to protocols approved by the Yale Animal Care and Use Committee.

Murine Challenges with Bacteria and Surgeries

CLP surgery was performed as described (Rittirsch et al., 2009). Mice were anesthetized using isoflurane inhalation, and the cecum was exteriorized through a peritoneal midline incision. Seventy-five percent of the cecum was ligated and punctured through and through with a 21G hypodermic needle. A small amount of fecal material was squeezed out, and the cecum was reinserted into the peritoneal cavity. After closing the abdomen in two layers, mice received 1 ml saline subcutaneously. Buprenorphine was injected every 12 hr for analgesia. Sham surgeries, including cecal exteriorization but without ligation and puncture, were performed as control. Survival and disease scores (from healthy/alert, via slightly lethargic [slightly delayed response to experimenter, slowed movement], and lethargic [significantly reduced response to experimenter, raised fur, slowed and reduced movement] to very lethargic [body shaking, hunchback, absence of evasion movements] and dead) were monitored several times daily. Body surface temperature was measured dorsally using an infrared thermometer. Murine catheter implant surgery was performed as described (Cassat et al., 2007). Wild-type mice were anesthetized using isoflurane inhalation, and a dorsal area was shaved. Following surface disinfection, a 3–4 mm incision was made on each mouse flank. Using a blunt probe to form subcutaneous pockets, 2 cm catheter tubing (BD Biosciences) was inserted into each cavity. Incisions were sutured, and approximately 5×10^6 CFUs of exponentially growing *S. aureus* SA113, washed and diluted in PBS, were injected through the skin into the lumen of the catheters. At 3 days after implant, the devices were removed, rinsed once, and then sonicated in PBS. The number of attached bacteria was determined by plating serial dilutions on agar plates. For monomicrobial infection, *iafgp*-expressing mice were infected with the *S. aureus* MRSA isolate USA300 JE2; 1.2×10^8 CFU logarithmic growth phase bacteria per mouse were applied intranasally in 50 μl PBS, and murine survival was monitored.

Mice were monitored at regular intervals for up to 36 hr for the following signs of moribund condition: sustained hypothermia (body temperature < 30°C for more than 1 hr, as measured by the infrared thermometer), lethargy, dehydration, change in color of mucous membranes, and labored breathing. We determined that mice showing more than three of the indicated signs were moribund and euthanized them promptly with CO_2.

Statistical Analysis

All experiments were repeated independently at least three times, if not noted otherwise. Statistical differences between groups were analyzed using Student's t test, one-way ANOVA, or two-way ANOVA with Tukey's or Sidak's posttest. Differences in survival were calculated using the log rank (Mantel-Cox) test. Contingency tables were analyzed with the chi-square test; $^*p < 0.05$, $^{**}p < 0.01$, and $^{***}p < 0.001$ were considered significant. Calculations, analysis, and graphing were performed using Excel 2007 (Microsoft), Prism 6.0 (GraphPad Software), and CorelDraw X4 (Corel). CFU data were logarithmically transformed before statistical analysis.

SUPPLEMENTAL INFORMATION

Supplemental Information includes five figures and can be found with this article online at http://dx.doi.org/10.1016/j.celrep.2014.09.034.

AUTHOR CONTRIBUTIONS

M.H., G.N., and E.F. designed the study. M.H., N.M.A., L.L., G.N., S.M., H.S., Z.S., J.M.-A., C.K., and W.W. performed experiments and analyzed data. H.A., L.C., and R.F. provided advice and helped plan experiments. M.H. and E.F. wrote the manuscript, and all the authors reviewed and edited the article. E.F. directed the overall investigations.

ACKNOWLEDGMENTS

We thank Kimberly Jefferson for bacterial strains and reagents; Andrew Hudson for help with the fruit fly colony; Timur Yarovinski for scientific discussions; and Kathleen Deponte, Ying Yang, Jingyi Pan, Michael Schadt, and Barry Piekos for technical assistance. This work was supported by grant AI41440 from the NIH to Erol Fikrig. Erol Fikrig and Richard Flavell are investigators with the Howard Hughes Medical Institute.

Received: May 28, 2014
Revised: July 26, 2014
Accepted: September 3, 2014
Published: October 16, 2014

REFERENCES

Allen, R.C., Popat, R., Diggle, S.P., and Brown, S.P. (2014). Targeting virulence: can we make evolution-proof drugs? Nat. Rev. Microbiol. *12*, 300–308.

Apidianakis, Y., and Rahme, L.G. (2009). Drosophila melanogaster as a model host for studying Pseudomonas aeruginosa infection. Nat. Protoc. *4*, 1285–1294.

Bouma, H.R., Henning, R.H., Kroese, F.G., and Carey, H.V. (2013). Hibernation is associated with depression of T-cell independent humoral immune responses in the 13-lined ground squirrel. Dev. Comp. Immunol. *39*, 154–160.

Boutilier, R.G. (2001). Mechanisms of cell survival in hypoxia and hypothermia. J. Exp. Biol. *204*, 3171–3181.

Bownes, M., Abrahamssen, N., Gilman, C., Howden, R., Martinez, A., and Slee, R. (1990). Book Reviews: Drosophila: A Laboratory Handbook. By Michael Ashburner. New York: Cold Spring Harbor Laboratory. 1989. Genet. Res. *56*, 71–73.

Brownstein, J.S., Holford, T.R., and Fish, D. (2003). A climate-based model predicts the spatial distribution of the Lyme disease vector Ixodes scapularis in the United States. Environ. Health Perspect. *111*, 1152–1157.

Carvajal-Rondanelli, P.A., Marshall, S.H., and Guzman, F. (2011). Antifreeze glycoprotein agents: structural requirements for activity. J. Sci. Food Agric. *91*, 2507–2510.

Cassat, J.E., Lee, C.Y., and Smeltzer, M.S. (2007). Investigation of Biofilm Formation in Clinical Isolates of Staphylococcus aureus. In Methicillin-Resistant Staphylococcus aureus (MRSA) Protocols, J. Yinduo, ed. (Totowa, NJ: Humana Press), pp. 113–126.

Christensen, G.D., Simpson, W.A., Younger, J.J., Baddour, L.M., Barrett, F.F., Melton, D.M., and Beachey, E.H. (1985). Adherence of coagulase-negative staphylococci to plastic tissue culture plates: a quantitative model for the adherence of staphylococci to medical devices. J. Clin. Microbiol. *22*, 996–1006.

Cramton, S.E., Gerke, C., Schnell, N.F., Nichols, W.W., and Götz, F. (1999). The intercellular adhesion (ica) locus is present in Staphylococcus aureus and is required for biofilm formation. Infect. Immun. *67*, 5427–5433.

Davies, P.L., and Sykes, B.D. (1997). Antifreeze proteins. Curr. Opin. Struct. Biol. *7*, 828–834.

Doucet, D., Walker, V.K., and Qin, W. (2009). The bugs that came in from the cold: molecular adaptations to low temperatures in insects. Cell. Mol. Life Sci. *66*, 1404–1418.

Garner, J., and Harding, M.M. (2010). Design and synthesis of antifreeze glycoproteins and mimics. ChemBioChem *11*, 2489–2498.

Griffith, M., and Yaish, M.W. (2004). Antifreeze proteins in overwintering plants: a tale of two activities. Trends Plant Sci. *9*, 399–405.

Huang, T., and Duman, J.G. (2002). Cloning and characterization of a thermal hysteresis (antifreeze) protein with DNA-binding activity from winter bittersweet nightshade, Solanum dulcamara. Plant Mol. Biol. *48*, 339–350.

Kim, T., and Kim, Y.J. (2005). Overview of innate immunity in Drosophila. J. Biochem. Mol. Biol. *38*, 121–127.

Long, W.B., 3rd, Edlich, R.F., Winters, K.L., and Britt, L.D. (2005). Cold injuries. J. Long Term Eff. Med. Implants *15*, 67–78.

Maki, D.G., Kluger, D.M., and Crnich, C.J. (2006). The risk of bloodstream infection in adults with different intravascular devices: a systematic review of 200 published prospective studies. Mayo Clin. Proc. *81*, 1159–1171.

Meyer, K., Keil, M., and Naldrett, M.J. (1999). A leucine-rich repeat protein of carrot that exhibits antifreeze activity. FEBS Lett. *447*, 171–178.

Neelakanta, G., Sultana, H., Fish, D., Anderson, J.F., and Fikrig, E. (2010). Anaplasma phagocytophilum induces Ixodes scapularis ticks to express an antifreeze glycoprotein gene that enhances their survival in the cold. J. Clin. Invest. *120*, 3179–3190.

Neelakanta, G., Hudson, A.M., Sultana, H., Cooley, L., and Fikrig, E. (2012). Expression of Ixodes scapularis antifreeze glycoprotein enhances cold tolerance in Drosophila melanogaster. PLoS ONE *7*, e33447.

Nehme, N.T., Quintin, J., Cho, J.H., Lee, J., Lafarge, M.-C., Kocks, C., and Ferrandon, D. (2011). Relative roles of the cellular and humoral responses in the Drosophila host defense against three gram-positive bacterial infections. PLoS ONE *6*, e14743.

Nishimura, S., Tsurumoto, T., Yonekura, A., Adachi, K., and Shindo, H. (2006). Antimicrobial susceptibility of Staphylococcus aureus and Staphylococcus epidermidis biofilms isolated from infected total hip arthroplasty cases. J. Orthop. Sci. *11*, 46–50.

Ramos, E.R., Reitzel, R., Jiang, Y., Hachem, R.Y., Chaftari, A.M., Chemaly, R.F., Hackett, B., Pravinkumar, S.E., Nates, J., Tarrand, J.J., and Raad, I.I. (2011). Clinical effectiveness and risk of emerging resistance associated with prolonged use of antibiotic-impregnated catheters: more than 0.5 million catheter days and 7 years of clinical experience. Crit. Care Med. *39*, 245–251.

Rittirsch, D., Huber-Lang, M.S., Flierl, M.A., and Ward, P.A. (2009). Immunodesign of experimental sepsis by cecal ligation and puncture. Nat. Protoc. *4*, 31–36.

Storey, K.B., and Storey, J.M. (2013). Molecular biology of freezing tolerance. Compr Physiol *3*, 1283–1308.

Triggs, A., and Knell, R.J. (2012). Interactions between environmental variables determine immunity in the Indian meal moth Plodia interpunctella. J. Anim. Ecol. *81*, 386–394.

Turk, E.E. (2010). Hypothermia. Forensic Sci. Med. Pathol. *6*, 106–115.

Venketesh, S., and Dayananda, C. (2008). Properties, potentials, and prospects of antifreeze proteins. Crit. Rev. Biotechnol. *28*, 57–82.

Vuong, C., Voyich, J.M., Fischer, E.R., Braughton, K.R., Whitney, A.R., DeLeo, F.R., and Otto, M. (2004). Polysaccharide intercellular adhesin (PIA) protects Staphylococcus epidermidis against major components of the human innate immune system. Cell. Microbiol. *6*, 269–275.

Walz, J.M., Memtsoudis, S.G., and Heard, S.O. (2010). Prevention of central venous catheter bloodstream infections. J. Intensive Care Med. *25*, 131–138.

Yaish, M.W., Doxey, A.C., McConkey, B.J., Moffatt, B.A., and Griffith, M. (2006). Cold-active winter rye glucanases with ice-binding capacity. Plant Physiol. *141*, 1459–1472.

Zhang, S., Wei, Y., and Pan, H. (2007). Transgenic rice plants expressing a novel antifreeze glycopeptide possess resistance to cold and disease. Z. Naturforsch., C, J. Biosci. *62*, 583–591.